ZnO-Coated Carbon Nanotubes: Flexible Piezoelectric Generators

Chia Jung Hu, Yu Hsien Lin, Chiung Wen Tang, Meng Yen Tsai, Wen Kuang Hsu, and Hsin Fu Kuo**

Wang et al. recently devised piezoelectric generators made of aligned ZnO nanowires and the Schottky barrier controlled output current was found to range from pA to a few nA.[1–3] In their study aligned oxide nanowires were deflected by an ultrasonic-wave-induced mechanical stress and the number of active nanowires that produce electricity was estimated to be 1000 wires cm^{-2}. However, the reported technique for generating piezoelectricity has disadvantages including: First, ceramics are brittle in nature and material fractures are inevitable with repeated deflections, thus reducing piezoelectric performance and reproducibility. Second, the design is complex and an accurate spacing with tolerance less than 1 μm is required between the electrode and the piezoelectric ZnO array. Third, the zigzag electrode induces various strain modes on the nanowires and thus the average power density is reduced. We present here an alternative approach for piezoelectric generation in which devices are constructed by coating carbon nanotubes (CNTs) with ZnO using atomic layer deposition (ALD). The study shows that the piezoelectric character does not fade away with repeated stress applications, and coating oxides remain intact because the flexible CNTs act as underlying cushions.[4] The average open-circuit voltage (V_{OC}) reaches a value as high as 1.6 V and the short-circuit current (I_{SC}) is 75 μA cm^{-2}, approximately a factor of 3000 greater than what was previously reported.[1] A Schottky barrier induced rectifying effect at the oxide/tube interface is also identified and accounts for the device polarity.

Figure 1 shows scanning electron microscopy (SEM) and transmission electron microscopy (TEM) images of ALD-treated CNT arrays and the oxide coating is evident. The nanotubes display different diameters in the upper and lower sections and SEM images from a microscope equipped with position marking software reveals 55–70 nm for the former and 20–30 nm for the latter (Figure 1b,c). The CNTs are graphite sheets rolled into seamless cylinders and conjugated surfaces do not accumulate charges upon SEM beam irradiation. Accordingly, the charging-induced bright-field fringe contrast in the upper section of the nanotube arrays (Figure 1a) must come from the insulating property, most likely from the coating ZnO. The nanotubes exhibit a core/shell structure after ALD treatment and the coating thickness lies between 30 and 35 nm (Figure 1d). The electron diffraction analysis reveals the coating to be a wurtzite structure (inset, Figure 1e). It is worth mentioning that the ALD diffusion depth is around 60 to 65 μm in the current study, and a prolonged ALD process from 200 to 800 cycles thickens the grain size by 40–50% along the *c*-axis and by 0.5% along the tube axis, which is consistent with a previous study.[4]

Based on the coated CNT arrays, three devices, named the C-, P-, and S-generators, were constructed for different purposes (see Experimental Section). **Figure 2**a shows a C-generator built for fatigue testing of the coating oxide upon repeated compression. First, the multifolding indicates that the coating did not greatly stiffen the CNTs and the array remained flexible along the tube axis (Figure 2b). Second, the average I_{SC} reached 75 μA cm^{-2} (Figure 2c) and was a factor of 3000 greater than previously reported data for oxide nanowires.[1] Third, detached oxides were not found after 200 compression cycles (C_y) and the I_{SC} was only lowered by 5% relative to the value observed at $C_y = 50$. At $C_y > 400$ the array flattening became obvious and was due to resilience-induced intertube sliding.[5] Strain formation of the coating oxides was limited and the I_{SC} was significantly reduced. Fourth, the oxides remained coated at $C_y = 400$ and the coating thickness revealed by SEM was 30–35 nm, similar to that for the pristine structure. The compression-induced array flattening may be overcome by filling the devices with a polymer that prevents intertube sliding. The second device, defined as a P-generator, was therefore made with polymer filled into intertube voids (see Experimental Section) and the coated nanotubes were arranged perpendicular to the electrode direction (**Figure 3**a). In addition to resistive CNTs, the silver electrodes were also connected to the coating ZnO, and carriers began to flow as a potential was established across the electrodes by oxide straining. Accordingly, the equivalent circuit of a P-generator resembles an electrical source and the nanotube resistors were connected in parallel (inset, Figure 3a); the former originates from stressed coating oxides and the latter from CNTs acting as carrier collectors. Due to the varied coating thickness along the tube axis, the oxides may deform non-uniformly and produce different current densities from tube to tube. The overall performance of a P-generator remains governed by the equivalent circuit approximation and can therefore be characterized by V_{OC}. At zero strain the linear current–voltage (*I*–*V*) profile confirms the resistive nature of the P-generators (Figure 3b). Upon twisting every 5 s (Figure 3c), the P-generator yielded

C. J. Hu, Y. H. Lin, C. W. Tang, Prof. W. K. Hsu, Dr. H. F. Kuo
Department of Materials Science and Engineering
National Tsing Hua University
Hsinchu, 30013, Taiwan
E-mail: wkhsu@mx.nthu.edu.tw; hsinfu@gmail.com
M. Y. Tsai
Instrumental Technology Research Center
National Applied Research Laboratories,
Hsinchu, 30076, Taiwan

DOI: 10.1002/adma.201100358

© 2011 WILEY-VCH Verlag GmbH & Co. KGaA, Weinheim

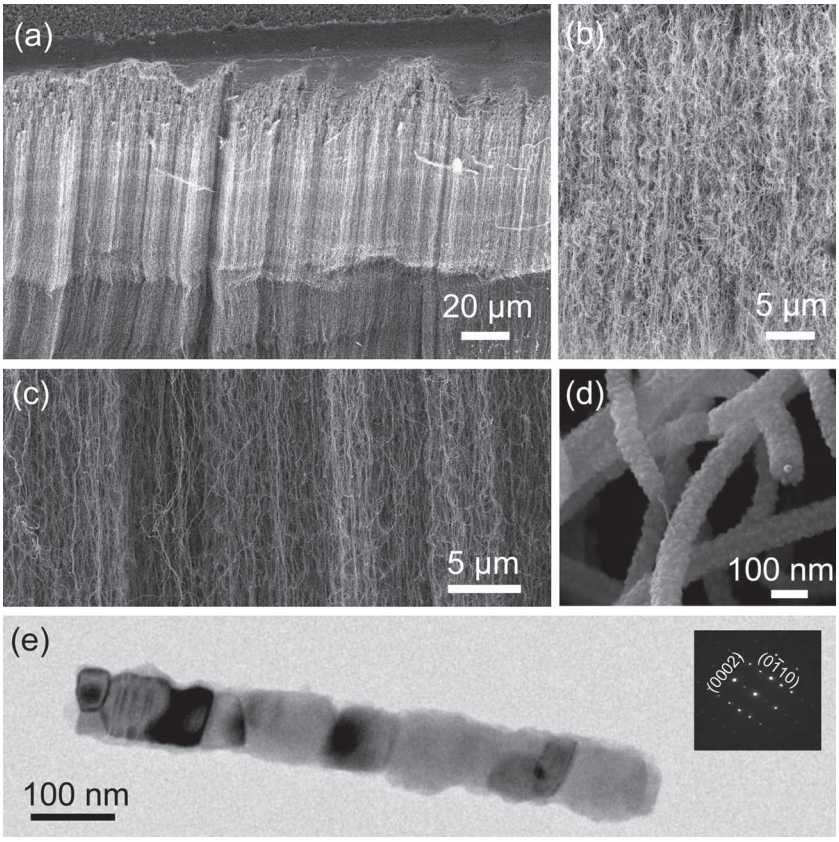

Figure 1. SEM images of a) ZnO-coated CNTs, b) a coated section, and c) a CNT section. d) A zoomed-in image of a ZnO-coated structure. e) TEM image of a coated CNT. The inset of (e) shows the electron diffraction patterns.

V_{OC} = 0.6–1.6 V (Figure 3d); the signal fluctuation came primarily from the instability of the manual exertion and did not increase with the twisting cycle (T_y). The protective polyvinyl alcohol (PVA) layer (see Experimental Section) began to fracture at T_y > 1200 and the observed decrease of V_{OC} was due to exposure and segregation of the coated nanotubes. Bending of the P-generator along the electrode direction produced a low V_{OC} and the reduced power output was due to the fact that such a stress mode primarily resulted in CNT displacement rather than deformation of the coating oxides (Figure 3a). Twisting of two P-generators connected in parallel gave V_{OC} = 0.6–1.9 V (Figure 3e), whereas the potential dropped to zero with an antiparallel connection (Figure 3f), which was attributable to cancellation of opposite V_{OC} values. The linear superposition test above confirmed that the observed V_{OC} truly comes from the generators and the contribution from artifacts or electrical noise from measurement system could be excluded.[6]

The S-generator was made by pasting conductive silver electrodes onto the coating and nanotube sections, and the equivalent circuit resembled an electrical source and nanotube resistors connected in series (**Figure 4**a). We therefore expected a Schottky barrier at the CNT/oxide interface (see panels (a,b) in the Supporting Information)[7–11] and the piezoelectric performance was evaluated according to the I_{SC} magnitude. Upon reverse bias application, the potential barrier increased and carrier passage was significantly reduced (panel (c), Supporting Information). In contrast, the reduced barrier at forward bias allowed carriers to flow (panel (d), Supporting Information). The rectifying effect was evident in the *I*–*V* profile at zero strain (Figure 4b). The coated nanotubes were then regularly bent at zero bias (Figure 4c) and I_{SC} was measured with respect to the device polarity, as shown in Figure 4d,e (insets). Current pulses emerged at the forward connections and the average I_{SC} was 18 μA cm^{-2} (Figure 4d). Exchange of electrical leads changed the sign of I_{SC}, whereas the magnitude of I_{SC} remained unchanged (Figure 4e). The switching polarity test again excluded the instrumental contribution to creation of I_{SC}.[6]

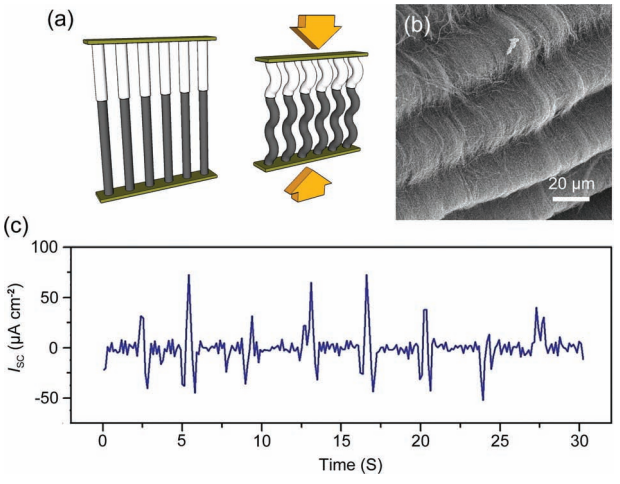

Figure 2. a) Piezoelectric generation by a C-generator upon compression, b) multifolding of a ZnO-coated nanotube array, and c) corresponding I_{SC} creation during each compression cycle.

Table 1 lists the power density ($P = IV/v$, where v is the volume of nanotube array) of the current devices and those previously reported. For the P-generator P reaches 36.8 μW cm^{-3}, which is a factor of 75 greater than that of oxide nanowires. Note that in our devices carriers are instantly transferred onto the conductive CNTs so that the power dissipation due to scattering by the oxide grain boundaries is limited,[12] which accounts for the improved P (i.e., $P_P >> P_S > P_{ZnO}$, where the subscript refers to the device type). $P_P >> P_S$ originates from the differentiated circuit resistance and is supported by the different profile slopes between Figures 3c and 4c. Compared to lead zirconate titanate (PZT), the P_P, however, is still lower by half and the underlying mechanism possibly involves the following factors. First, the piezoelectric character originates only from the ZnO coating and the actual oxide content in the current devices is much lower than that of oxide nanowires and PZT. Second, a small fraction of the created carriers may be trapped by CNT

© 2011 WILEY-VCH Verlag GmbH & Co. KGaA, Weinheim

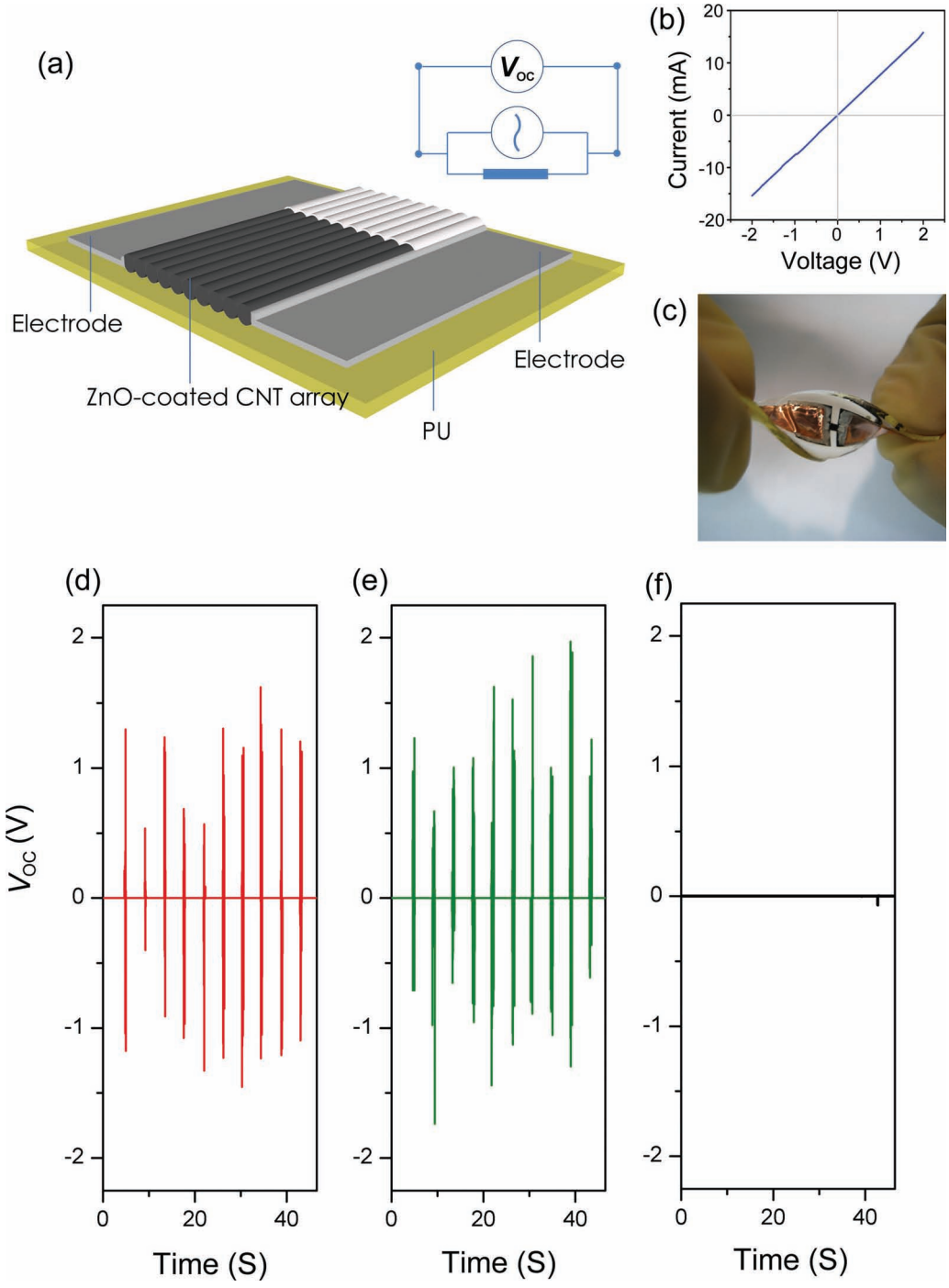

Figure 3. a) Structure of a P-generator. Inset: corresponding circuit elements. b) *I–V* profile obtained from a P-generator at zero strain. c) Device twisting. d) The V_{OC} produced by a single P-generator and e,f) two P-generators connected in parallel and antiparallel, respectively.

defects, which act as radical scavengers.[13] Third, carriers leak through the protective hydrophilic PVA, and the V_{OC} and I_{SC} are therefore reduced. We find that the I_{SC} reduction as a function of bending cycle (B_y) is very low and lies below 1% at $B_y \approx$ 500 to 1000. This is becuase the CNT-bending-induced strain on the coating oxides is relatively low compared with Figure 2a.

Next, we estimated the energy converting efficiency (ECE), which is defined as the ratio between the generated electrical work and the deformation-created potential energy. The calculation was carried out according to the S-generator structure. The nanotube deformation can be considered as tensile strain (ε) because the substrate thickness greatly exceeds the array height and the nanotube length is much shorter than the curvature radius of bending (Supporting Information). The empirical model was employed and equation is written as $\varepsilon = h/2R$, where h is the substrate thickness (1 mm) and R is the curvature

© 2011 WILEY-VCH Verlag GmbH & Co. KGaA, Weinheim

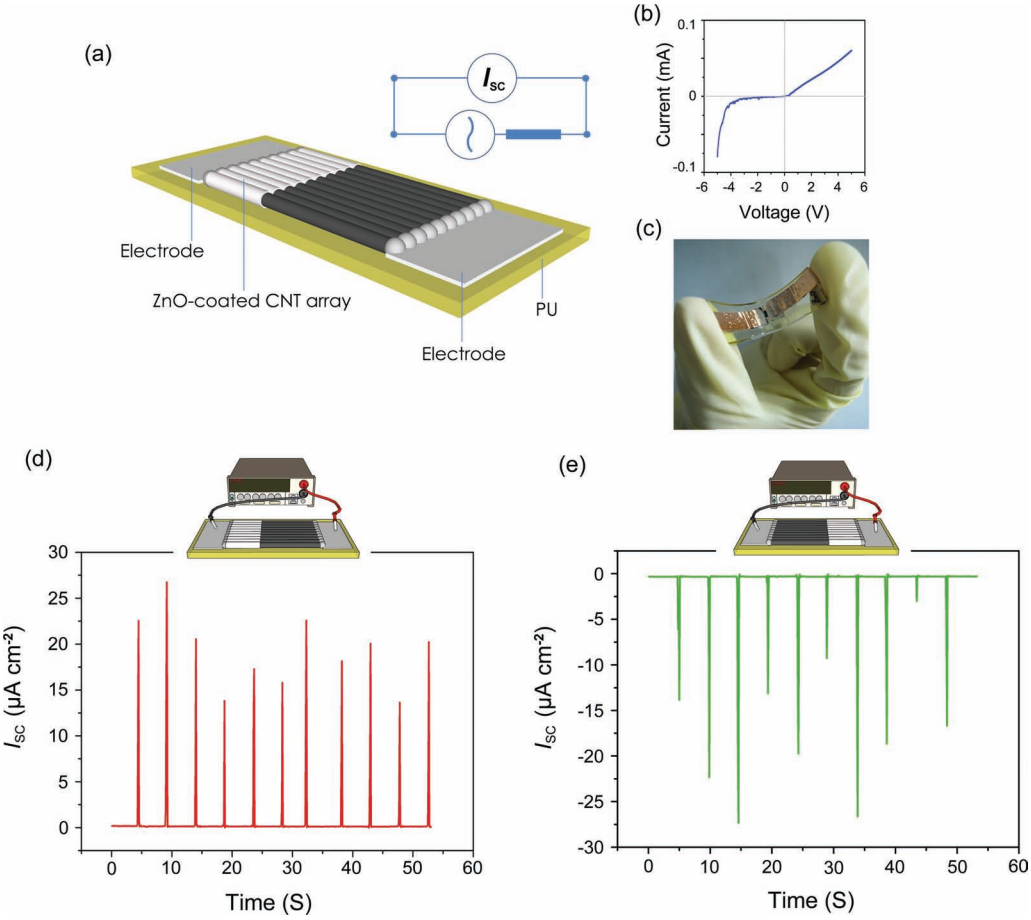

Figure 4. a) Structure of an S-generator. Inset: corresponding circuit elements. b) *I–V* profile obtained from an S-generator at zero strain. c) Device bending. d,e) I_{SC} creation with forward and reverse connections, respectively.

radius. The elastic strain energy (U_M) of the nanotube arrays is therefore given by $U_M = Y\varepsilon^2 v/2$, where the Young's modulus is experimentally determined ($Y = 2.26$ MPa) and v is the array volume (= 1 mm^3). The fraction contributed by the coating oxide ($U_{M,\,ZnO}$) is given by $U_{M,\,ZnO} = U_M\,[Y_{ZnO}/(Y_{ZnO} + Y_{CNT})]$, where Y_{CNT} is the Young's modulus of CNTs (= 1.8 TPa)[14] and Y_{ZnO} is the Young's modulus of ZnO (= 60 GPa).[15] The table in the Supporting Information shows the related parameters of efficiency at R = 15 and 30 mm, and the corresponding ε values have been calculated to be 3.3% and 1.75%, respectively. Compared to single crystal nanowires the ECE of our devices is lower, which is attributable to ALD-created polycrystalline oxides (Figure 1e).[4] The S-generator, however, has the following advantages. First, the bending does not cause CNT segregation and four-terminal experiments carried out on different S-generators yield similar *I–V* profiles (Figure 4c). Second, the interfacial Schottky barrier allows carriers to flow unidirectionally; an energy harvesting system constructed from S-generators therefore needs no supplementary rectifiers. However, the question remains as to how CNTs prevent the coating from fracturing. Inhibition of oxide detachment requires i) a sufficient binding at oxide/tube interface and ii) a uniform dispersion of the load. The former also means that carriers produced at the oxide can be successfully transferred onto CNT, as is evident here by I_{SC} creation. In Figure 2a, we see that coated CNTs buckle in response to compression and the process somewhat resembles a concertina in operation.[16] Accordingly, the mechanical energy may be stored through spring compression (Figure 2a), which is supported as follows. First, the nanotube conductivity is sensitive to strain formation and the large I_{SC} creation here seems to suggest the absence of a localized strain-induced resistance increase. Second, the localized strain formation is also avoided, as the spring slightly buckles in response to device twisting and bending (Figures 3 and 4). Third, CNT arrays are porous and intertube voids allow the stressed nanotubes to relax. Based on SEM inspection and the Brunauer–Emmett–Teller (BET) measurement revealed pore volume of CNT arrays (0.209–0.21 cm^3 g^{-1}), the average intertube separation is found to be 0.1–0.2 μm, exceeding the radius of CNT gyration before the onset of the buckling mode.[17] In other words, array compression does not lead to tube–tube squeezing.

Table 1. Power density of current and reported work.

	P-generator	S-generator	ZnO nanowire[1]	PZT cantilever[18]
P [μW cm^{-3}]	36.8	0.54	0.5	70

© 2011 WILEY-VCH Verlag GmbH & Co. KGaA, Weinheim

In summary, we have fabricated various piezoelectric generators by coating ZnO onto aligned CNT arrays and the generated I_{SC} is 3 to 6 orders of magnitude greater than previously reported data for ZnO nanowires. The ZnO coating does not significantly stiffen nanotubes and the constant creation of I_{SC} and V_{OC} indicates the absence of stress-induced oxide fracture. CNTs behave as carrier collectors and improve device conductivity and P.

Experimental Section

A silicon wafer used as the sample collector was placed in an alumina furnace heated to 1400 K and multiwalled CNTs (MWCNTs) were grown by injecting a ferrocene-dissolved xylene solution (1:50, 100 c.c.) into the furnace. MWCNT arrays were then transferred into an ALD reactor for ZnO coating, with diethylzinc and water used as precursors. The deposition rate was controlled at 0.7 Å per cycle and the reaction was carried out at 300 K.[4] The coating oxide was analyzed by scanning electron microscopy (SEM, JEOL JSM-6500F) and transmission electron microscopy (TEM, JEOL JEM-3000F). The ALD-treated nanotube arrays were then thermally filled with poly-para-xylylene (tradename: parylene) to form a robust composite structure using the following procedure. First, the parylene dimers were vaporized at 150 °C and the vapor was mixed with methylene in a stainless steel chamber connected to the pyrolysis furnace. Second, the chamber temperature was increased to 680 °C to decompose the gas mixture into stable monomeric diradical para-xylyene and the monomers were subsequently redirected into a pyrolysis furnace at room temperature. This led to polymerization in CNT arrays and produced composites consisting of aligned MWCNTs coated with parylene.[16] Three different piezoelectric devices were fabricated as follows. First, the top and bottom faces of the as-grown CNT array (2 mm × 2 mm × 1 mm) were pasted with conductive silver as the electrical connections. This device, defined as the C-generator, was built to test the fatigue of coating oxide upon repeated compression and the polymer filling was therefore excluded in the fabrication procedure. Second, a polymer-filled CNT composite was sliced into a thin structure (0.5 mm × 2 mm) and the electrical connections were made to both the oxide and CNT sections simultaneously (Figure 3a). The device was placed onto a flexible polyurethane substrate and was subsequently covered with PVA to prevent dust and moisture contamination. This device was defined as the P-generator and piezoelectricity was generated by twisting the polyurethane substrate. Third, the third device defined as the S-generator was made using a similar method to the P-generator, except the silver electrodes were pasted onto the oxide and CNTs, respectively, and the piezoelectric performance was characterized through the bending mode (Figure 4a,b). The stress-induced piezoelectricity was recorded in situ using a power supply (Keithley-2400) with the background noise controlled at ± 0.5 nA and the experiments were carried out under ambient conditions.

Supporting Information

Supporting Information is available from the Wiley Online Library or from the author.

Acknowledgements

C.J.H. and Y.H.L. contributed equally to this work. The authors thank the National Science Council of Taiwan for the financial support (NSC-99–2112-M-007–014-MY2).

Received: January 28, 2011
Revised: March 7, 2011
Published online: May 13, 2011

[1] X. D. Wang, J. H. Song, J. Liu, Z. L. Wang, *Science* **2007**, *316*, 102.
[2] Y. Qin, X. D. Wang, Z. L. Wang, *Nature* **2008**, *451*, 809.
[3] R. S. Yang, Y. Qin, L. M. Dai, Z. L. Wang, *Nat. Nanotechnol.* **2009**, *4*, 34.
[4] S. Y. Lu, C. W. Tang, Y. H. Lin, H. F. Kuo, Y. C. Lai, M. Y. Tsai, H. Ouyang, W. K. Hsu, *Appl. Phys. Lett.* **2010**, *96*, 231915.
[5] S. H. Syue, C. T. Hsu, U. S. Chen, H. J. Chen, W. K. Hsu, H. C. Shih, *Carbon* **2009**, *47*, 1239.
[6] Z. L. Wang, *Adv. Funct. Mater.* **2008**, *18*, 3553.
[7] R. P. Gao, Z. W. Pan, Z. L. Wang, *Appl. Phys. Lett.* **2001**, *78*, 1757.
[8] S. Hasegawa, S. Nishida, T. Yamashita, H. Asahi, *J. Ceram. Process Res.* **2005**, *6*, 245.
[9] R. Martel, T. Schmidt, H. R. Shea, T. Hertel, P. Avouris, *Appl. Phys. Lett.* **1998**, *73*, 2447.
[10] M. Shiraishi, M. Ata, *Carbon* **2001**, *39*, 1913.
[11] W. S. Su, T. C. Leung, C. T. Chan, *Phys. Rev. B* **2007**, *76*, 235418
[12] Z. L. Wang, X. Y. Kong, Y. Ding, P. Gao, W. L. Hughes, R. Yang, Y. Zhang, *Adv. Funct. Mater.* **2004**,*14*, 943
[13] Y. F. Li, C. I. Hung, C. C. Li, W. Chin, B. Y. Wei, W. K. Hsu, *J. Mater. Chem.* **2009**, *19*, 6761.
[14] M. M. J. Treacy, T. W. Ebbesen, J. M. Gibson, *Nature* **1996**, *381*, 678.
[15] M. J. Mayo, R. W. Siegel, Y. X. Liao, W. D. Nix, *J. Mater. Res.* **1992**, *7*, 973.
[16] W. K. Hsu, H. Y. Chu, T. H. Chen, T. W. Cheng, W. Fang, *Nanotechnology* **2008**, *19*135304.
[17] S. Y. Lu, W. K. Hsu, *ChemPhysChem* **2005**, *6*, 1040.
[18] S. Roundy, P. K. Wright, J. Rabaey, *Comput. Commun.* **2003**, *26*, 1131.

© 2011 WILEY-VCH Verlag GmbH & Co. KGaA, Weinheim